

The partition coefficient of alloying elements and its influence on the pitting corrosion resistance of 15Cr-2Ni duplex stainless steel

Jianquan Wan^{a,b}, Yan Lou^a, Haihui Ruan^{b,*}

^a College of Mechatronics and Control Engineering, Shenzhen University, Shenzhen 518060, China

^b Department of Mechanical Engineering, The Hong Kong Polytechnic University, Hung Hom, Kowloon, Hong Kong, China

Abstract

This work investigates the influence of heat treatment parameters including annealing temperature, time and cooling rate on the partition coefficient of alloying elements between ferrite and austenite phases, and obtains the pitting corrosion resistance comparison between ferrite and austenite phases. The partition coefficient varies with the annealing temperature, time and cooling rate, which is associated with the change of ferrite volume fraction. When ferrite volume fraction increases, the partition coefficient becomes more uniform and close to 1. The contrast of pitting corrosion resistance between ferrite and austenite phases varies with the change of the partition coefficient of alloying elements.

Key words: Duplex stainless steel; Partition coefficient; Pitting corrosion resistance

* Corresponding author: Tel./fax: + 852 2766 6648.

E-mail address: haihui.ruan@polyu.edu.hk

1. Introduction

Duplex stainless steel (DSS), consisting of body-centered cubic ferrite (δ) and face-centered cubic austenite (γ), combines most of the beneficial properties from austenitic stainless steel and ferritic stainless steel such as excellent mechanic property and corrosion resistance, good weldability [1-3]. Therefore, DSS is widely used for various applications such as submarine pipelines, pressure vessels, and nuclear power facilities [4-6], and alloy diffusion is important for the industrial application of DSS by affecting its corrosion property [7].

The δ and γ phases exhibit a varying affinity for different alloying elements, which are called austenite stabilizers such as Ni and N and ferrite stabilizers such as Cr and Mo. The partitioning degree of alloying elements between δ and γ phases is calculated into the partition coefficient, which impacts much on the corrosion resistance of DSS [8, 9].

To reduce the material cost, Cr and Ni can be replaced partially by Al and Mn respectively. Such replacement leads to the novel 15Cr-xAl-2.0Ni-yMn DSS, which, in comparison with conventional DSS alloys, have much less Cr and Ni contents and similar mechanical performance and corrosion resistance [10]. Conventional research focused more on how to improve the mechanical property but less on corrosion property, so DSS is usually recommended to have δ to γ phase ratio close to 1:1 through some proper heat treatment [7-10]. Very few research can be found on the influence of heat treatment on the pitting corrosion resistance of DSS. The additions of Al and Mn further complicate the empirical relation between corrosion resistance and the compositions of Cr and Ni. The important question we may ask is: what is the role of the partition coefficient of alloying elements in affecting the pitting corrosion resistance of DSS.

Cortie *et al.* [8] investigated the effect of temperature and nitrogen on the partitioning of alloy elements in 22Cr DSS by experimental and empirical means. Zhang *et al.* [9] investigated the influence of microstructure and elemental partitioning on the pitting corrosion resistance of δ and γ phases in DSS welding joints. Bernhardsson [11] used thermodynamic data to reckon that the pitting corrosion resistance of the alloy can be optimized by selecting a proper annealing temperature. Solomon and Devine [12] discussed that how the proportion of δ and γ phases influences the pitting corrosion resistance of DSS. These studies indicate that alloying elements partitioning varies with different conditions and affects the pitting corrosion resistance of DSS.

Solution treatment changes the concentration of alloying elements in δ and γ phases and therefore changes the pitting corrosion resistance [13-16]. For a DSS sample, heat treatment parameters such as annealing temperature, time and cooling rate, may lead to significantly different pitting corrosion resistance, which needs a detailed study. This work is motivated by the consideration that the non-equilibrium phase transformation, which is ubiquitous in producing DSS, should be thoroughly explored so that the segregation behaviour of alloying elements can be well controlled and used. An attempt was made to describe the effect of heat treatment parameters such as annealing temperature, time and cooling rate on the partition coefficient of alloying elements between δ and γ phases and resultant pitting corrosion resistance of 15Cr-2Ni-2Al-11Mn DSS.

2. Experimental

The research is based on 15Cr-2Al-2Ni-11Mn alloy, and the specific chemical composition after spectroscopic analysis of the casting is shown in Table 1. The raw materials were melted in an electric arc furnace and then fast solidified into a copper mould at room temperature, which

resulted in about 70% δ phase in the as-cast alloy [17]. The metallograph and the XRD pattern of the casting were shown in Fig.1(a) and Fig.1 (b), respectively.

The samples were then subjected to isothermal annealing at 750~1150 °C for 1~480 min followed by furnace cooling of about 5 °C/min [18], air cooling (8~20°C/s [19, 20]) or water quenching (500~2200 °C/s [20, 21]), respectively. The details of heat-treatment schedule is listed in Table 2.

The concentration of the alloying elements in δ and γ phases was measured using energy dispersive X-ray spectroscopy (EDS) with the energy of incoming electron 20 kV, which was equipped in a scanning electron microscopy (JEOL JSM-6490)) system. The EDS count of elemental concentration in each adjacent δ and γ phases was used to calculate the single partition coefficient K_i for element i , which is defined as $K_i = C_i^\delta / C_i^\gamma$ where C_i^δ and C_i^γ represent the concentration of element i in the adjacent δ and γ phases respectively. And the average value of 10 single K_i obtained from different areas with adjacent δ and γ phases is taken as final partition coefficient K .

The pitting corrosion resistance was investigated using potentiodynamic polarization curves obtained by the standard pitting corrosion test following ASTM G48-03 [22]. The potentiodynamic polarization tests were conducted in a 200 ml solution of 3.5 wt.% NaCl at 25 °C with the three-electrode setup, in which a Pt foil, a saturated calomel electrode, and the sample are the auxiliary, the reference, and the working electrodes, respectively. Polarization test of each specimen was performed at least three times using an EG&G Princeton Applied Research Potentiostat / Galvanostat Model 273A. Before the scan was initiated, the samples were immersed in the solution for 10 min to stabilize the open-circuit potential (OCP).

Potentiodynamic polarization curves were recorded from -0.5 V to 1.5 V with respect to the OCP. The value of potential where the current increases sharply from the passive current level was used to represent the pitting corrosion potential. Uniform corrosion tests were conducted using a 6 wt.% ferric chloride solution at 25 °C, which is in accordance with the standard ASTM G48-03.

3. Result and discussion

3.1 The effect of annealing temperature

The partition coefficients (K) of major alloying elements in the casting ingot are all in the range of 0.95~1.05 as shown in Table 3, since the ingot is obtained by fast solidification. Fig. 2(a) shows the variations of partition coefficient of DSS samples heated at 750~1150 °C for (I) 30 min and (II) sufficiently long time followed by water quenching, respectively. The effect of annealing temperature on K value was found to be significant, such as that the strong partitioning of Ni into γ phase decreases with increasing temperature as reported in [8, 23].

For case (I), which is a conventional annealing method, K deviates away from the uniform line $K=1$ in 750~950 °C and then approaches $K=1$ at the temperature higher than 950 °C. For case II, sufficiently long time means that the quenched δ content does not change further with longer annealing time, and DSS samples achieve the isothermal equilibrium state [17]. The annealing time for the DSS samples achieving the isothermal equilibrium state at 750, 850, 950, 1050, and 1150 °C were 240, 180, 60, 15 and 5 min, respectively. In case II, K approaches the uniform line $K=1$ monotonically as the annealing temperature increases. Fig. 2(b) shows the variations of the volume fraction of δ phase ϕ_δ against annealing temperature T for (I) 30 min and (II) sufficiently long time followed by water quenching, respectively. Through the

comparison between Fig.2(a) and Fig.2(b), it is noted that the variation of the partition coefficient K exhibits the same trend as that of δ content. Atamert and Cortie [8, 24] reported that the element partitioning between the primary phases becomes more uniform when the solution temperature increases. It should be the case for the casting alloy solidified by air cooling, which the phase constitution in the casting is close to the thermal equilibrium state due to the low cooling rate. So the δ content increases with annealing temperature in conventional annealing time of 30 min [10, 25]. In this work, the casting contains 70% δ phase content, which deviates far away from the thermo-equilibrium state. Thus, the δ phase content dependent on annealing temperature exhibits the trend as shown in Fig.2 (b) [17]. Therefore, it can be concluded more exactly that the partition coefficient K becomes more uniform with the increased δ phase content.

3.2 The effect of annealing time

Fig. 3 shows the experiment result and linear fitting curves on the variation of partition coefficient K when DSS samples were heated at (a) 750 °C, (b) 950 °C, and (c) 1050 °C followed by water quenching, respectively. It is noted that the partition coefficients of Cr and Al increase while those of Ni and Mn decrease with the annealing time, finally levels off after 240 min for 750 °C, 60 min for 950 °C and 30 min for 1050 °C. It should be noted that δ -to- γ phase transformation occurs at temperature below 1050 °C and the durations needed for reaching isothermal phase-equilibrium state at the three temperatures are 240 min for 750 °C, 60 min for 950 °C and 15 min for 1050 °C respectively [17]. To simply explain the isothermal phase-equilibrium state, Fig.4(a) and Fig.4 (b) show the metallographs of DSS samples heated at 1050 °C for 15 and 30 min followed by water quenching respectively, and the same volume fraction of δ phase were obtained. The δ volume fraction decreases with annealing time within 15 min. From 15 min to 30 min, δ volume fraction does not change.

Above comparison indicates that the composition homogenization occurs after the phase transformation completed, which suggests that the migration of phase boundary may be faster than the diffusion of alloying elements.

3.3 The effect of cooling rate

Fig. 5 shows the variation of alloying elements of DSS samples heated at 750~1150 °C for 30 min followed by water quenching, air cooling and furnace cooling, respectively. The partition coefficient of water quenched group is closer to 1 than those of air cooling and furnace cooling groups. The comparison of the partition coefficient between water quenching and furnace cooling was analysed herein due to their significant difference. All DSS alloys were solidified ferritically and then transformed partially to γ during cooling [16]. Therefore, the δ volume fraction obtained by furnace cooling is lower than that of water quenching. As concluded in section 3.1, K becomes more uniform with the increased δ phase content. Therefore, K values of Cr and Al after furnace cooling are higher than those of water quenching, while K values of Ni and Mn after furnace cooling are lower than those of water quenching. The deviation magnitude of the partition coefficient between furnace cooling and water quenching at 1050 ~1150 °C is much larger than that of below 1050 °C as shown in Fig. 5. It is consistent with the trend of experiment result that δ is much more transformed to γ when the DSS sample is cooled from the temperature higher than 1050 °C than that of below 1050 °C as shown in Fig. 6. It is also reported in [26] that the partition coefficient of alloying elements Cr, Mo, Ni and N is influenced by γ phase content in DSS.

3.4 Improve the corrosion resistance

Polarization test was carried out to investigate the pitting corrosion resistance of DSS samples. Pitting resistance equivalent number (PREN) is widely used to predict the pitting corrosion resistance and it correlates with the chemical composition of stainless steel. Higher PREN is generally in accord with better pitting corrosion resistance in most stainless steels. For the current resource-saving DSS, PREN is redefined for considering both the beneficial promotion of Al [27] and the detrimental influence of Mn [10, 28] on the pitting corrosion resistance as follows:

$$\text{PREN} = \text{wt.\% Cr} + 2.5 \text{ wt.\% Al} - 0.75 \text{ wt.\% Mn} + 3.3 \text{ wt.\% Mo}$$

Five samples were chosen to examine the pitting corrosion resistance of γ and δ phases. The DSS samples are coded as (1#) 1000-30-a, (2#) 1000-15-a, (3#) 750-30-w, (4#) 750-15-w and (5#) 1150-15-a, which indicate the DSS samples heated at 1000 °C for 30 min followed by air cooling, 1000 °C for 15 min followed by air cooling, 750 °C for 30 min followed by water quenching, 750 °C for 15 min followed by water quenching, 1150 °C for 15 min followed by air cooling, respectively. Fig. 7 (a) shows the representative polarization curves of 1~5# DSS samples in 3.5 wt.% NaCl aqueous solution at 25 °C, and the pitting potential values are 5# > 3# > 1# > 2# ~ 4# as listed in the Table 4. According to the specific chemical composition of δ and γ phases, the ratios of PREN value ($R_{\delta/\gamma}$) of the five samples are 14.40/8.10, 10.48/12.35, 12.53/11.76, 10.53/11.31, 13.72/10.76, respectively. The pitting corrosion resistance of 1#, 3# and 5# should be dependent on the pitting corrosion resistance of γ , while that of 2# and 4# is δ . So the theoretical sequence of the pitting corrosion resistance of DSS samples should be 3# > 5# > 4# ~ 2# > 1#, which is not consistent with that of the experiment result. The pitting corrosion resistance of DSS bulk is partially affected by the microstructure, particularly the contact area between the δ and γ phases/grains [28]. As it is well known that annealing temperature becomes

the biggest parameters for coarsening the grain size when it is higher than 950~1000 °C [29, 30], so the pitting corrosion resistance of δ and γ phases does not decide the pitting potential of the bulk at high temperature. DSS samples 1# and 2# have the same volume fraction of δ phase [17], but the grain size of 1# is much larger than that of 2# due to longer annealing time at 1000 °C. Thus, the contact area between δ and γ phases of 1# is less than that of 2#, and it can be the cause that the pitting potential value of 1# is higher than that of 2#. This case was also reported in [28]. While for low temperature, such as 750 °C case of 3# and 4#, the pitting corrosion resistance of δ and γ phases is consistent with the pitting potential of the bulk. To confirm above analysis, DSS samples heated at 850°C were further investigated. Fig.7(b) shows the representative polarization curves of DSS samples heated at 850°C for 30, 90 and 180 min followed by water quenching, respectively. The pitting potential of the bulk decreases with annealing time, while the PREN ratio value ($R_{\delta/\gamma}$) increases with annealing time from 30~180 min.

The metallographs of the samples after polarization test are shown in Fig. 8. It shows that the phase which was etched first for 1#, 3# and 5# is γ while that for 2# and 4# is δ . Two parameters of annealing time and temperature were investigated from this comparison. First, the effect of annealing time on the contrast of corrosion resistance between δ and γ phases is concluded from the comparison of samples 1# & 2# and 3# & 4#. Fig. 3 indicates that longer annealing time increases the concentration of Cr and Al and reduces the concentration of Mn in the δ phase at annealing temperature 750 and 1000 °C. Therefore, the $R_{\delta/\gamma}$ value of 1# is higher than that of 2#, and that of 3# is higher than that of 4#. It can be concluded that the longer annealing time, at the temperature inducing δ -to- γ transformation, leads to the increase of Cr and Al and decrease of Mn in δ phase, which improves the corrosion resistance of δ phase. Secondly, the effect of annealing temperature is concluded from the comparison of samples 2# and 5#. The γ -to- δ phase

transformation occurs at 1150 °C, which can be concluded from Fig.2(b) [17]. It leads to even lower content of Cr at 1150 °C compared to that of 1000 °C in the γ phase of DSS sample within short annealing time. Therefore, the γ phase becomes the weaker phase in pitting corrosion resistance than that of δ phase in DSS sample 5#.

4. Application on making the porous materials

The above investigation indicates that even with the same chemical composition, different heat treatments can bring about distinct contrast of the corrosion resistance between γ and δ phases, which was also reported in [9, 26]. One possible application is then to produce porous stainless steel by etching off a primary phase.

To demonstrate the possibility, uniform corrosion test was carried out with the DSS samples heated at 1100 °C for 30 min followed by furnace cooling. These DSS samples consist approximately 50/50 γ and δ phases, and exhibit nearly equiaxed phase morphology as shown in Fig. 9(a). After checking the chemical composition of γ and δ phases by SEM-EDS, the PREN contrast $R_{\delta/\gamma}$ was obtained as 1.43, which suggests that the pitting corrosion resistance of γ phase is much weaker than that of δ phase. These DSS samples were polished to thickness of 300 μm and then immersed in the solution of 3.5 wt.% NaCl for 6~120 h, respectively. Their metallographs were obtained as shown in Fig.9 (b), (c) and (d). It is noted that the etching rate of γ phase was not apparent until 48 h and then accelerated.

Therefore, the result indicates that the feasibility to produce porous stainless steel by etching off a primary phase in DSS, if the contrast of pitting corrosion resistance $R_{\delta/\gamma}$ between δ and γ deviates significantly from unity. It can be achieved by adjusting the annealing time and temperature for the DSS samples.

5. Conclusion

The influence of heat treatment parameters including annealing temperature, time and cooling rate on the partition coefficient of alloying elements between δ and γ phases was investigated and found to be useful to vary the corrosion resistance comparison between δ and γ phases of DSS. The main findings are:

1. The partition coefficient of alloying elements between δ and γ phases varies with the annealing temperature, time and cooling rate, which are correlated with the variation of δ phase volume fraction. When the δ phase volume fraction increases, the partition coefficient becomes more uniform and close to 1.
2. With the annealing time increases, the partition coefficients of Cr and Al increase while those of Ni and Mn decrease, finally levels off after the DSS sample reaching isothermal phase-equilibrium state.
3. The pitting corrosion resistance of δ and γ phases does not decide that of DSS bulk. The microstructure, particularly obtained at high temperature, exhibits impact on the pitting corrosion resistance of DSS bulk.
4. Longer annealing time is beneficial for improving the pitting corrosion resistance of δ phase if the annealing temperature leads to δ -to- γ phase transformation in DSS. Higher annealing temperature, at which γ -to- δ phase transformation occurs in DSS samples, can rapidly increase the pitting corrosion resistance of δ phase.
5. This work suggests the way to develop single-phase porous stainless steel through etching by controlling the heat treatment condition to achieve strong contrast of pitting corrosion resistance between δ and γ phases.

Acknowledgement

This work was supported by the Early Career Scheme (ECS) of the Hong Kong Research Grants Council (Grant No. 25200515), the Departmental General Research Funds (G-UA2L) of Hong Kong Polytechnic University, and National Natural Science Foundation of China (Grant No.51675347). We are grateful for the support.

Reference

- [1] Y. Wang, B. Yang, J. Han, F. Dong, Y. Wang, Localized corrosion of thermally aged cast duplex stainless steel for primary coolant pipes of nuclear power plant, *Procedia Engineering*, 36 (2012) 88-95.
- [2] S. Herenu, I. Alvarez-Armas, A. Armas, The influence of dynamic strain aging on the low cycle fatigue of duplex stainless steel, *Scripta materialia*, 45 (2001) 739-745.
- [3] H. Miyamoto, T. Mimaki, S. Hashimoto, Superplastic deformation of micro-specimens of duplex stainless steel, *Materials Science and Engineering: A*, 319 (2001) 779-783.
- [4] H. Luo, C. Dong, K. Xiao, X. Li, Characterization of passive film on 2205 duplex stainless steel in sodium thiosulphate solution, *Applied surface science*, 258 (2011) 631-639.
- [5] F. Zanotto, V. Grassi, A. Balbo, C. Monticelli, F. Zucchi, Stress corrosion cracking of LDX 2101® duplex stainless steel in chloride solutions in the presence of thiosulphate, *Corrosion Science*, 80 (2014) 205-212.
- [6] H. Farnoush, A. Momeni, K. Dehghani, J.A. Mohandesi, H. Keshmiri, Hot deformation characteristics of 2205 duplex stainless steel based on the behavior of constituent phases, *Materials & Design*, 31 (2010) 220-226.
- [7] P. Williams, R. Faulkner, Chemical volume diffusion coefficients for stainless steel corrosion studies, *Journal of materials science*, 22 (1987) 3537-3542.
- [8] M. Cortie, J. Potgieter, The effect of temperature and nitrogen content on the partitioning of alloy elements in duplex stainless steels, *Metallurgical Transactions A*, 22 (1991) 2173-2179.
- [9] Z. Zhang, H. Jing, L. Xu, Y. Han, L. Zhao, J. Zhang, Influence of microstructure and elemental partitioning on pitting corrosion resistance of duplex stainless steel welding joints, *Applied Surface Science*, 394 (2017) 297-314.
- [10] J. Wan, Q. Ran, J. Li, Y. Xu, X. Xiao, H. Yu, L. Jiang, A new resource-saving, low chromium and low nickel duplex stainless steel 15Cr-xAl-2Ni-yMn, *Materials & Design*, 53 (2014) 43-50.
- [11] J. Charles, S. Bernhardsson, Duplex Stainless Steels'91. Vol. 1, Beaune, France, 28-30 Oct. 1991, (1991) 1991.
- [12] T.M.D. H.D. Solomon, Proceedings of conference on Duplex Stainless Steels, ASM, Metal park, OH, 1983.
- [13] J.K.L. Lai, K.W. Wong, D.J. Li, Effect of solution treatment on the transformation behaviour of cold-rolled duplex stainless steels, *Materials Science and Engineering: A*, 203 (1995) 356-364.
- [14] V.S. Moura, L.D. Lima, J.M. Pardal, A.Y. Kina, R.R.A. Corte, S.S.M. Tavares, Influence of microstructure on the corrosion resistance of the duplex stainless steel UNS S31803, *Materials Characterization*, 59 (2008) 1127-1132.
- [15] T. Karahan, H. Ertek Emre, M. Tümer, R. Kaçar, Strengthening of AISI 2205 duplex stainless steel by strain ageing, *Materials & Design*, 55 (2014) 250-256.
- [16] J.-O. Nilsson, Super duplex stainless steels, *Materials science and technology*, 8 (1992) 685-700.
- [17] J. Wan, H. Ruan, J. Wang, S. Shi, Exploiting the non-equilibrium phase transformation in a 15Cr-2Ni-2Al-11Mn resource-saving duplex stainless steel, *Materials & Design*, 114 (2017) 433-440.
- [18] F. Martín, C. García, Y. Blanco, M.L. Rodríguez-Mendez, Influence of sinter-cooling rate on the mechanical properties of powder metallurgy austenitic, ferritic, and duplex stainless steels sintered in vacuum, *Materials Science and Engineering: A*, 642 (2015) 360-365.
- [19] T. Takei, M. Yabe, F.-G. Wei, Effect of cooling condition on the intergranular corrosion resistance of UNS S32506 duplex stainless steel, *Corrosion Science*, 122 (2017) 80-89.
- [20] Z. Xu, Y. Zhang, Quench rates in air, water, and liquid nitrogen, and inference of temperature in volcanic eruption columns, *Earth and Planetary Science Letters*, 200 (2002) 315-330.

- [21] A. Bardelcik, C.P. Salisbury, S. Winkler, M.A. Wells, M.J. Worswick, Effect of cooling rate on the high strain rate properties of boron steel, *International Journal of Impact Engineering*, 37 (2010) 694-702.
- [22] G. ASTM, 48-03. Standard test methods for pitting and crevice corrosion resistance of stainless steels and related alloys by use of ferric chloride solution, West Conshohocken, PA, United States, (2003).
- [23] S. Atamert, J.E. King, Elemental partitioning and microstructural development in duplex stainless steel weld metal, *Acta Metallurgica et Materialia*, 39 (1991) 273-285.
- [24] S. Atamert, J. King, Elemental partitioning and microstructural development in duplex stainless steel weld metal, *Acta metallurgica et materialia*, 39 (1991) 273-285.
- [25] J. Li, Z. Zhang, H. Chen, X. Xiao, J. Zhao, L. Jiang, New Economical 19Cr Duplex Stainless Steels, *Metallurgical and Materials Transactions A*, 43 (2012) 428-436.
- [26] L. Weber, P. Uggowitzer, Partitioning of chromium and molybdenum in super duplex stainless steels with respect to nitrogen and nickel content, *Materials Science and Engineering: A*, 242 (1998) 222-229.
- [27] F. Hull, Delta Ferrite and Martensite formation in stainless steels, *Welding journal*, 52 (1973) 193.
- [28] Y. Jang, S. Kim, J. Lee, Effect of different Mn contents on tensile and corrosion behavior of CD4MCU cast duplex stainless steels, *Materials Science and Engineering: A*, 396 (2005) 302-310.
- [29] X. Yuan, L. Chen, Y. Zhao, H. Di, F. Zhu, Influence of annealing temperature on mechanical properties and microstructures of a high manganese austenitic steel, *Journal of Materials Processing Technology*, 217 (2015) 278-285.
- [30] C. Zhao, R. Song, L. Zhang, F. Yang, T. Kang, Effect of annealing temperature on the microstructure and tensile properties of Fe-10Mn-10Al-0.7C low-density steel, *Materials & Design*, 91 (2016) 348-360.

List of Captions

Table 1 The specific chemical compositions of 15Cr-2Ni DSS (wt.%)

Table 2 Heat treatment schedule of 15Cr-2Ni DSS samples

Table 3 Concentration (wt.%) of major alloying elements in the δ and γ phases of the casting

Table 4 The pitting corrosion potential values of DSS samples 1# ~ 5# (a saturated calomel electrode as reference)

Fig. 1 (a) The metallograph and (b) the XRD pattern of the casting

Fig. 2 (a) Variations of partition coefficient of DSS samples heated at 750~1150 °C for (I) 30 min and (II) sufficiently long time followed by water quenching. (b) Variations of δ volume fractions of DSS samples heated at 750~1150 °C for (I) 30 min and (II) sufficiently long time followed by water quenching.

Fig. 3 Experiment result and linear fitting curves on the variation of partition coefficient of DSS samples heated at (a) 750 °C for 15~300 min and (b) 950 °C for 3~75 min followed by water quenching respectively, and (c) 1050°C for 10~60 min followed by water quenching, respectively. The shaded area refers to the composition homogenization period.

Fig. 4 Metallograph of DSS samples heated at 1050°C for (a) 15 and (b) 30 min followed by water quenching, respectively.

Fig. 5 Variations of partition coefficient of alloying elements (a) Cr and Al (b) Ni and Mn when DSS samples heated at 750~1150 °C for 30 min followed by water quenching, air cooling and furnace cooling, respectively.

Fig. 6 Variations of δ phase of DSS samples heated at 750~1150 °C for 30 min followed by water quenching, air cooling and furnace cooling, respectively

Fig.7 The representative polarization curves of DSS samples in 3.5 wt.% NaCl aqueous solution at 25 °C (a) samples 1~5# and (b) samples heated at 850 for 30, 90 and 180 min respectively followed by water quenching

Fig.8 Metallographs of DSS samples heated at 1000 °C for (a) 1#-30 min and (b) 2#-15 min followed by air cooling, 750 °C for (c) 3#-30 min and (d) 4#-15 min followed by water quenching, and (e) 5#-1150 °C for 15 min followed by air cooling after polarization test.

Fig.9 Metallographs of DSS samples heated at 1100 °C for 30 min followed by furnace cooling (a) and its metallographs after uniform corrosion test for (b) 48 h (c) 72h and (d)120 h at 25 °C.

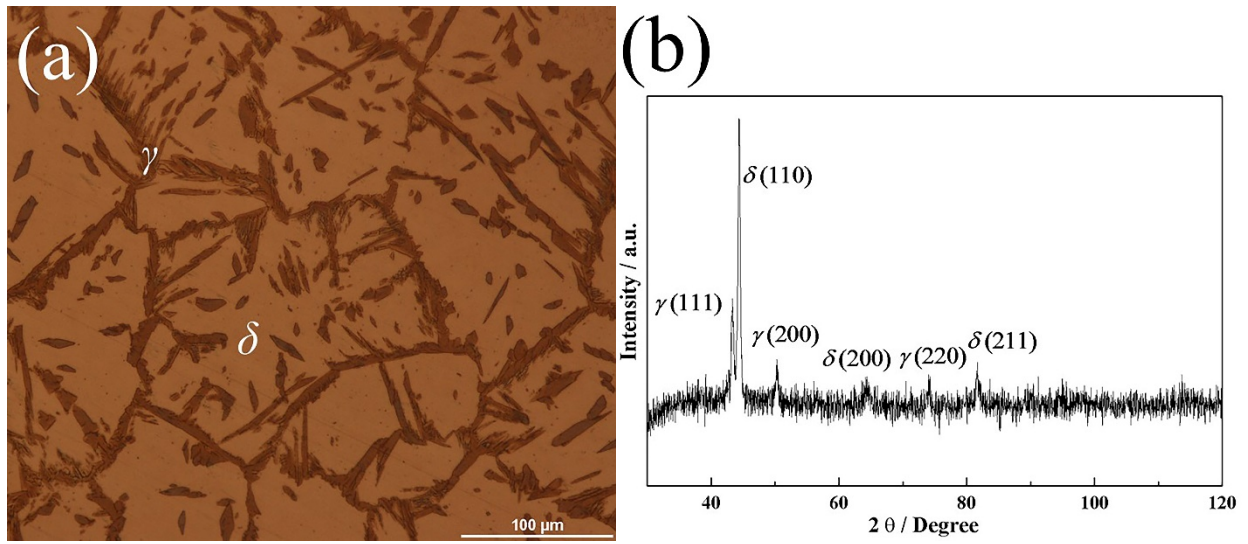


Fig. 1 (a) The metallograph and (b) the XRD pattern of the casting

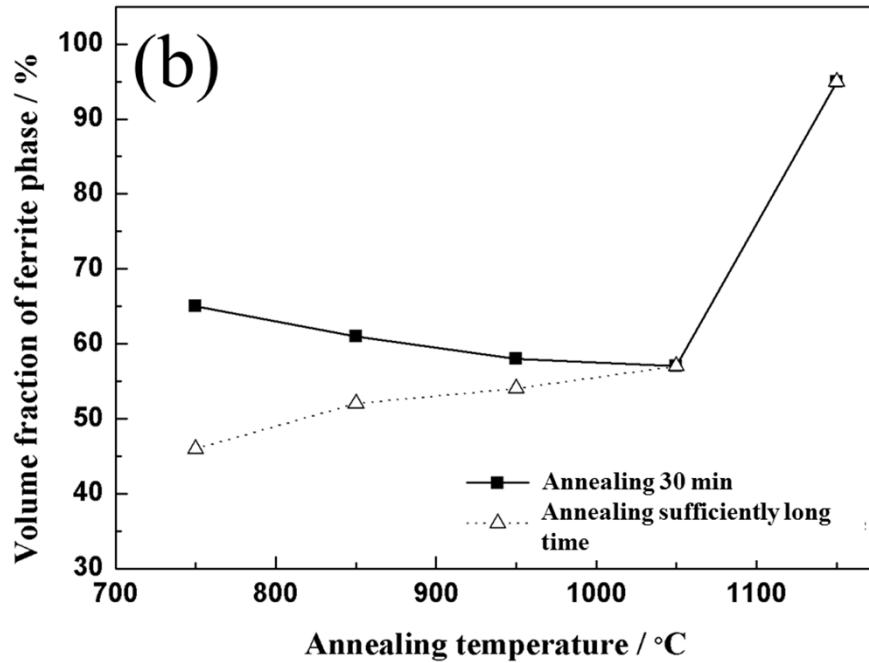
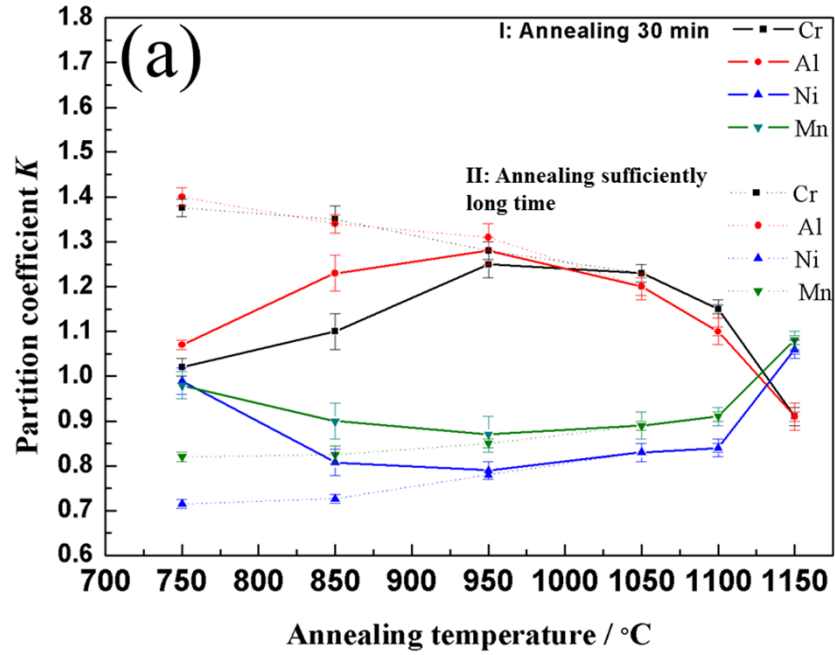


Fig. 2(a) Variations of partition coefficient of DSS samples heated at 750~1150 °C for (I) 30 min and (II) sufficiently long time followed by water quenching, respectively. (b) Variations of δ volume fractions of DSS samples heated at 750~1150 °C for (I) 30 min and (II) sufficiently long time followed by water quenching, respectively.

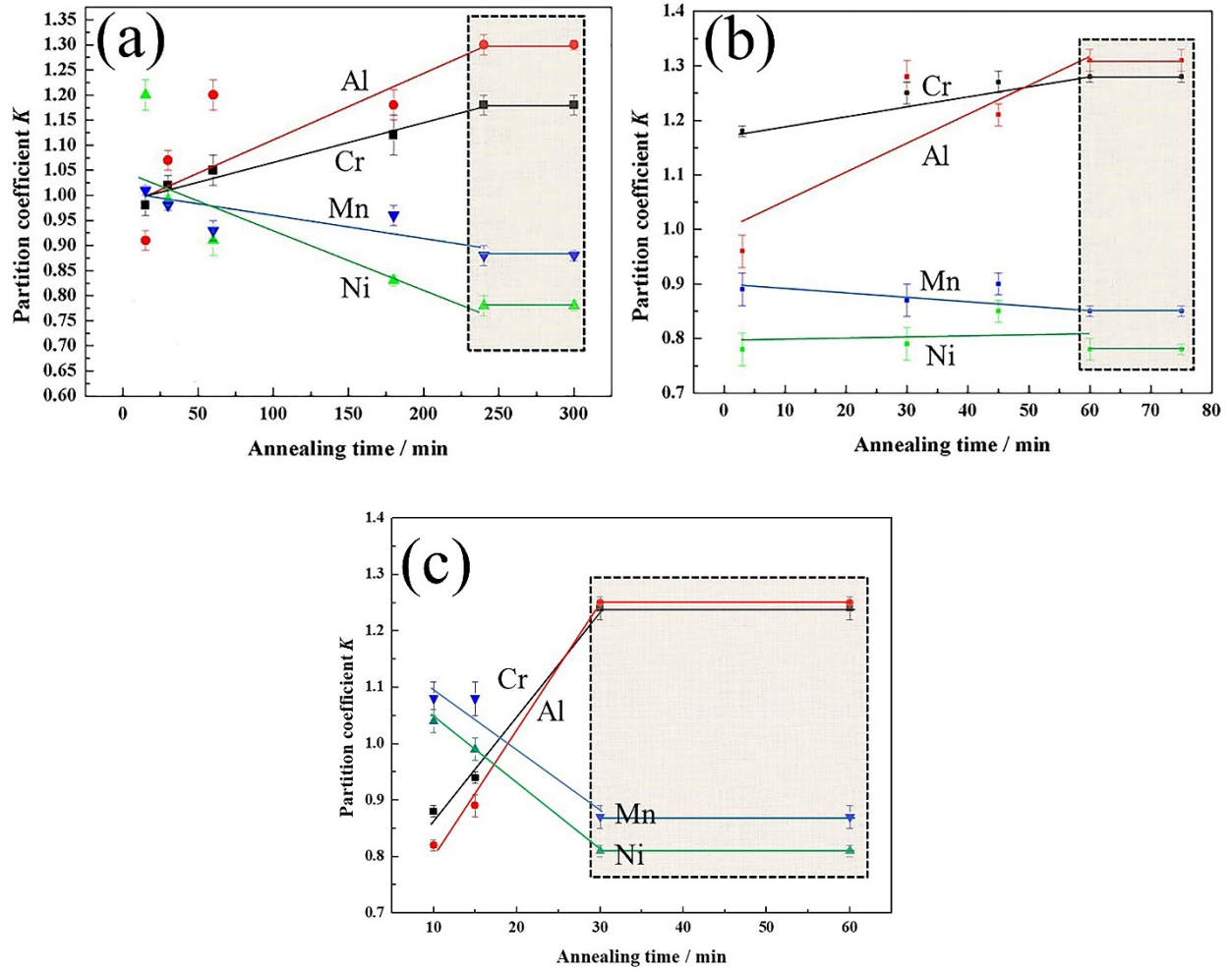


Fig. 3 Experiment result and linear fitting curves on the variation of partition coefficient of DSS samples heated at (a) 750 °C for 15~300 min and (b) 950 °C for 3~75 min and (c) 1050°C for 10~60 min followed by water quenching, respectively. The shaded area refers to the composition homogenization period.

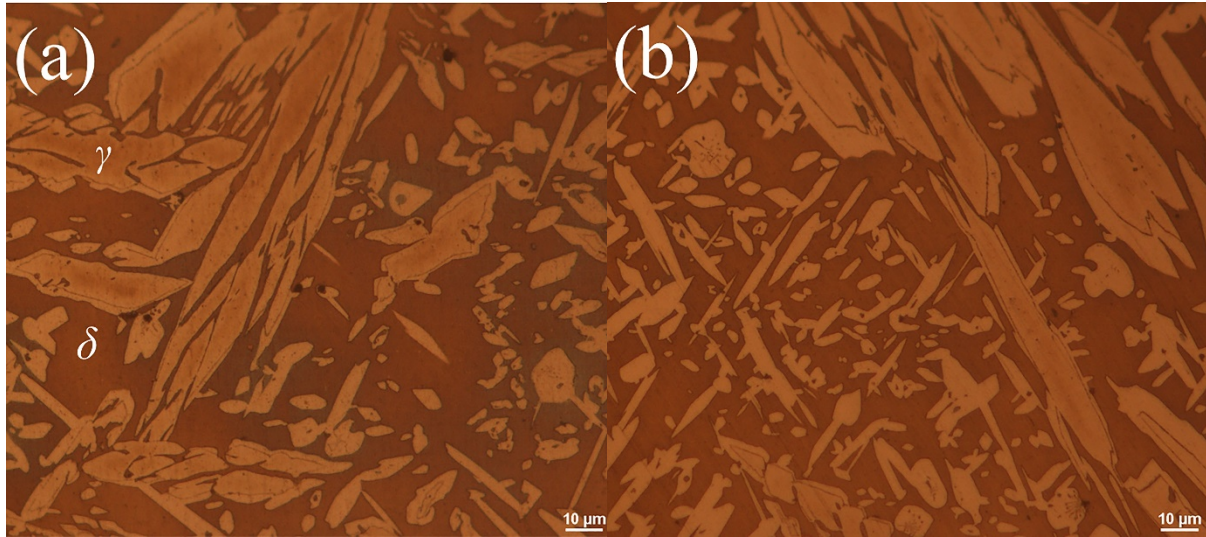


Fig. 4 Metallograph of DSS samples heated at 1050°C for (a) 15 and (b) 30 min followed by water quenching, respectively.

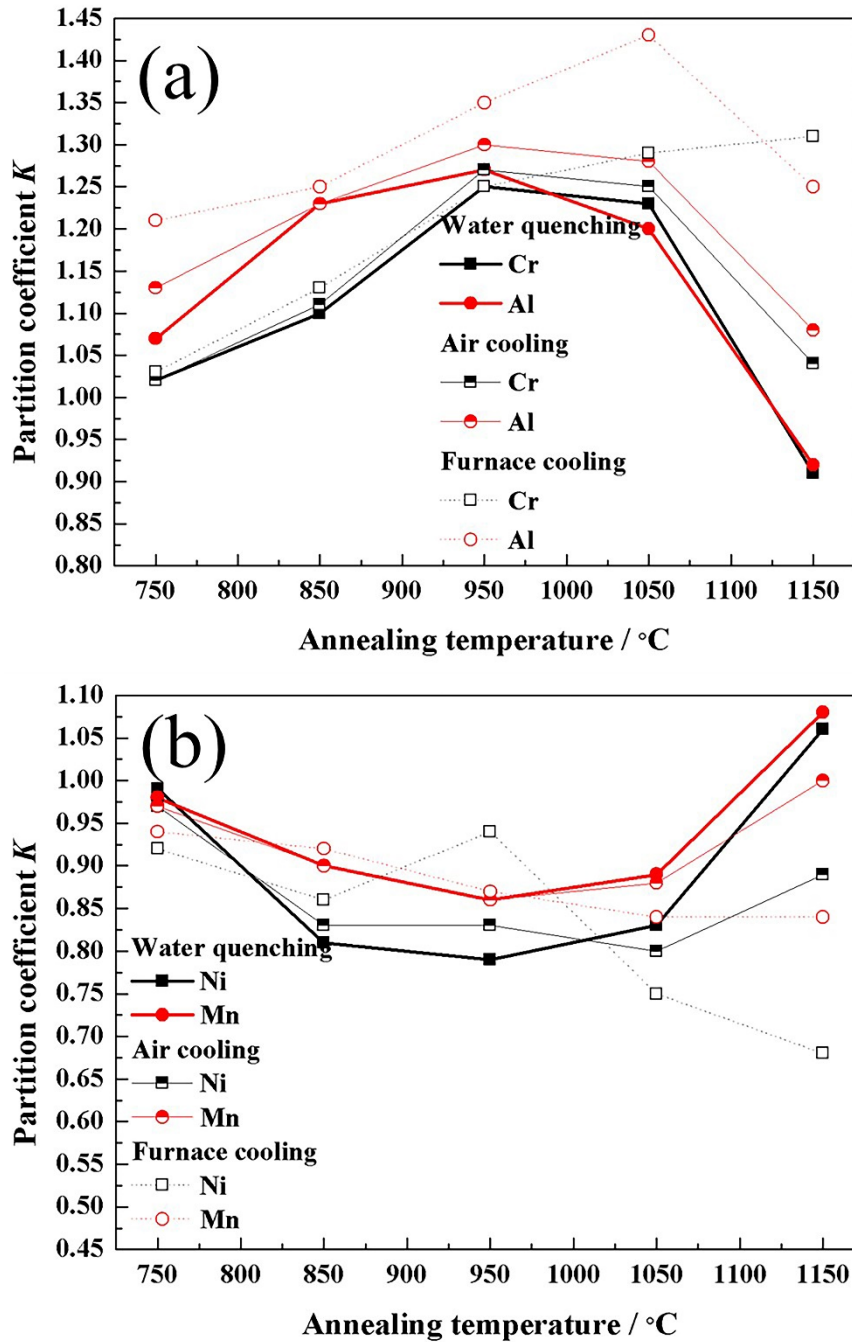


Fig. 5 Variations of partition coefficient of alloying elements (a) Cr and Al (b) Ni and Mn when DSS samples heated at 750~1150 °C for 30 min followed by water quenching, air cooling and furnace cooling, respectively.

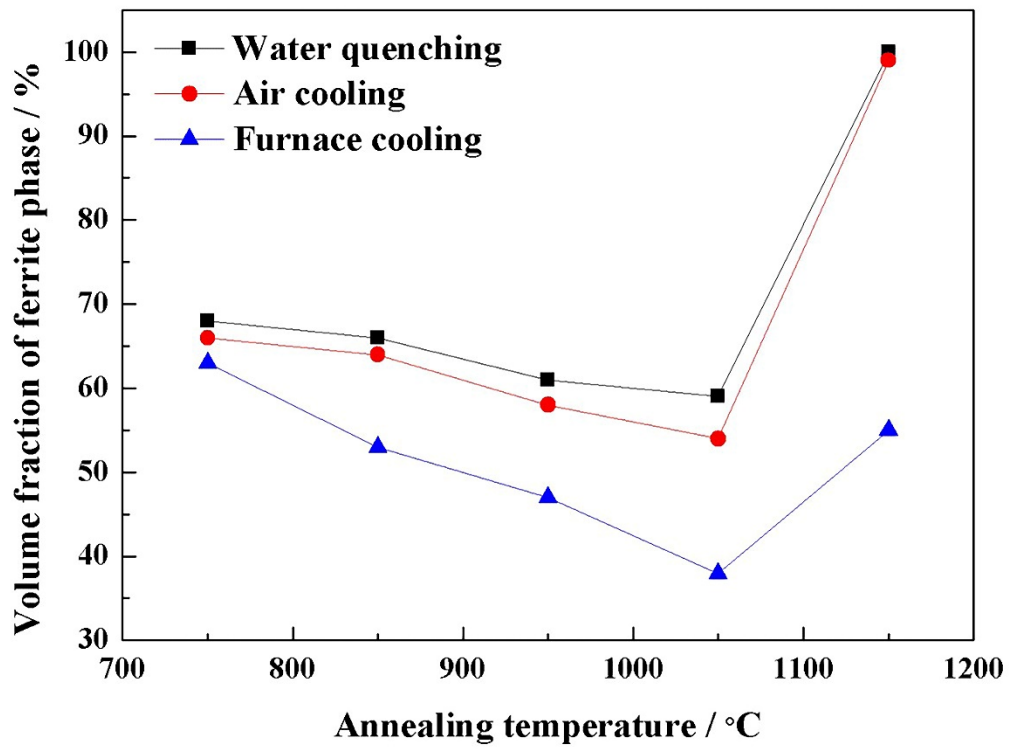


Fig. 6 Variations of δ phase of DSS samples heated at 750~1150 °C for 30 min followed by water quenching, air cooling and furnace cooling, respectively.

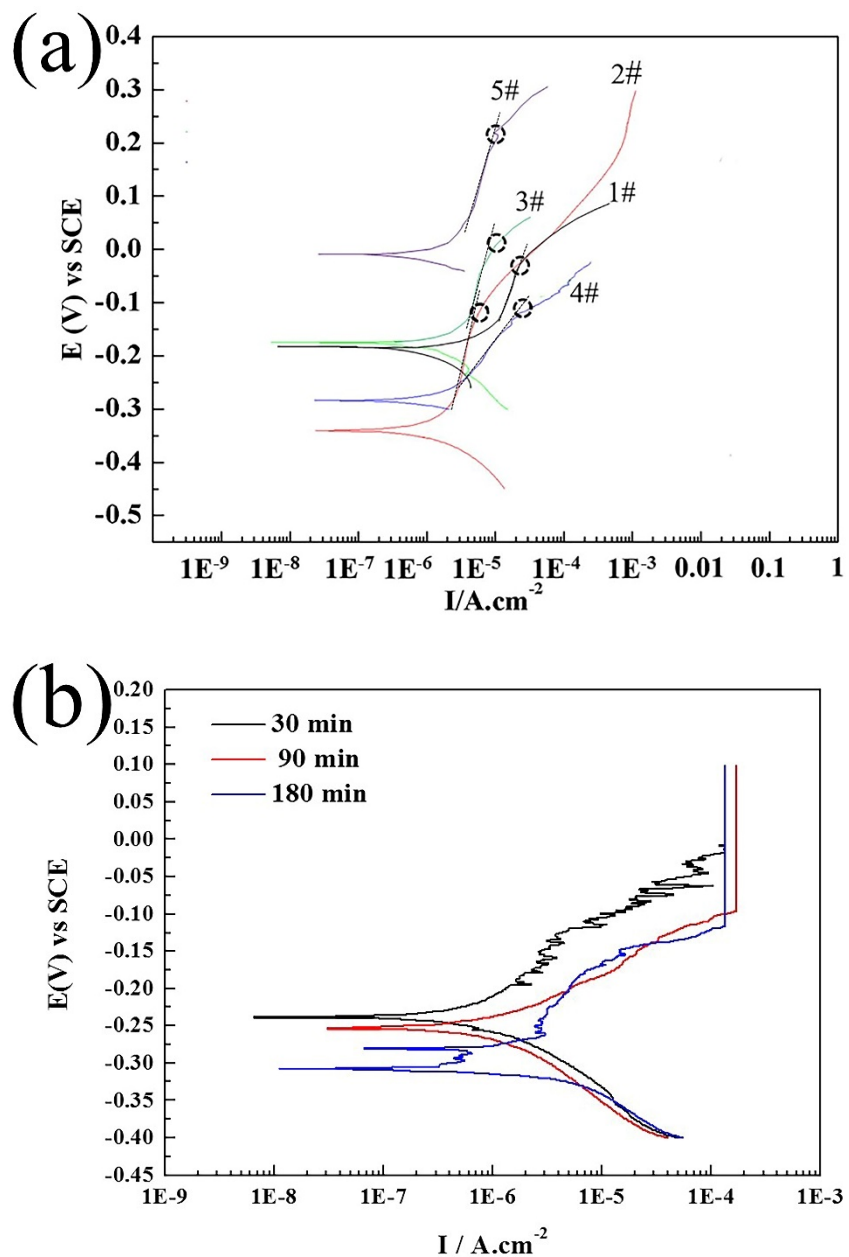


Fig.7 The representative polarization curves of DSS samples in 3.5 wt.% NaCl aqueous solution at 25 °C (a) samples 1~5# and (b) samples heated at 850 for 30, 90 and 180 min respectively followed by water quenching

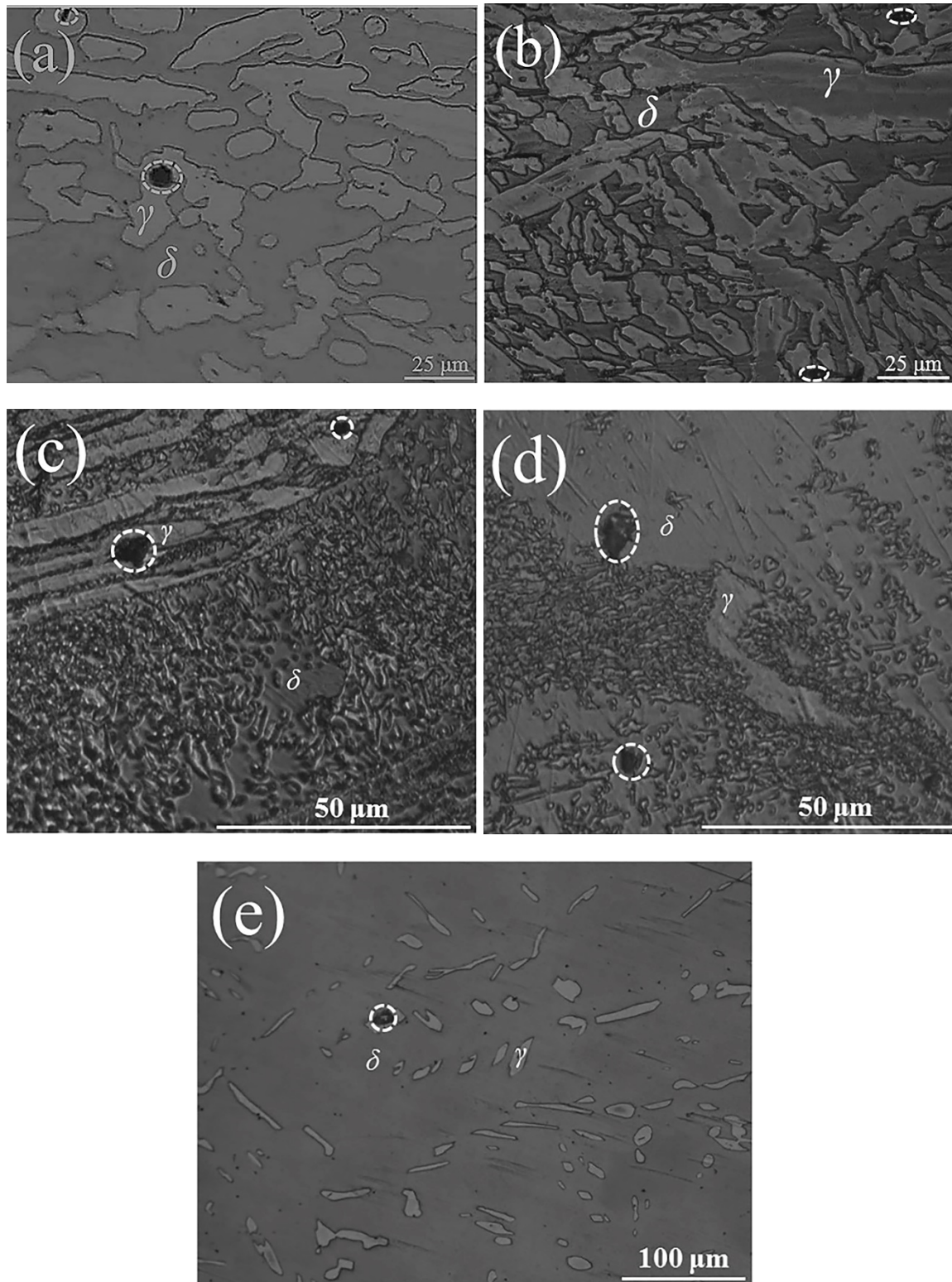


Fig.8 Metallographs of DSS samples heated at 1000 °C for (a) 1#-30 min and (b) 2#-15 min followed by air cooling, 750 °C for (c) 3#-30 min and (d) 4#-15 min followed by water quenching, and (e) 5#-1150 °C for 15 min followed by air cooling after polarization test.

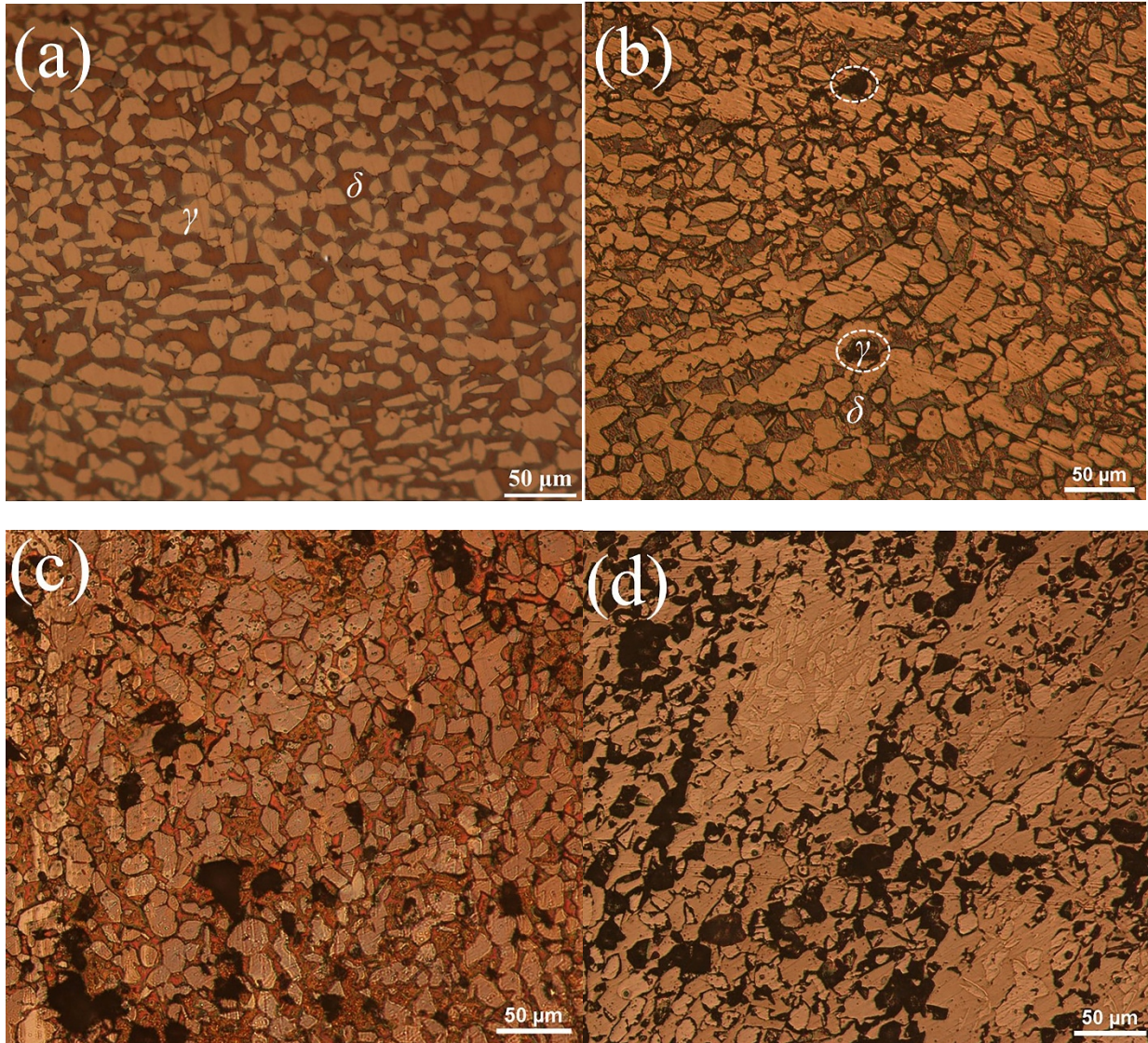


Fig.9 Metallographs of DSS samples heated at 1100 °C for 30 min followed by furnace cooling (a) and its metallographs after uniform corrosion test for (b) 48 h (c) 72h and (d)120 h at 25 °C.

Table 1 The specific chemical compositions of 15Cr-2Ni DSS (wt.%)

Element	Fe	Cr	Al	Ni	Mn	C
Wt.%	Balance	15.27	1.96	2.04	11.05	0.02

Table 2 Heat treatment schedule of 15Cr-2Ni DSS samples

Temp., °C	Time/min												
	3	10	15	30	60	90	120	150	180	210	240	300	480
750			■	■	■	■	■	■	■	■	■	■	■
850			■	■	■	■	■	■	■	■	■		
950	■	■	■	■	■	■	■						
1000	■	■	■	■	■	■	■						
1050	■	■	■	■	■	■	■						
1150	■	■	■	■	■	■							

Table 3 Concentration (wt.%) of major alloying elements in the δ and γ phases of the casting.

	Cr	K	Al	K	Ni	K	Mn	K
Ferrite	15.81		2.03		2		12.63	
Austenite	15.56	1.02	1.94	1.05	1.97	1.02	13.31	0.95

Table 4 The pitting corrosion potential values of DSS samples 1# ~ 5# (a saturated calomel electrode as reference)

DSS samples	1#	2#	3#	4#	5#
Pitting corrosion potential (mv)	-38	-120	25	-120	200
Error (mv)	4	10	3	8	5